

UNIVERSITY OF CALIFORNIA
SANTA CRUZ

AN LSTM RECURRENT NETWORK FOR STEP COUNTING

A report submitted in partial satisfaction of the
requirements for the degree of

MASTER OF SCIENCE

in

COMPUTER SCIENCE

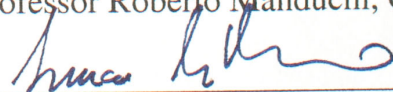
by

Ziyi Chen

December 2017

The Report of Ziyi Chen
is approved:

Professor Roberto Manduchi, Chair



Professor Luca de Alfaro, Reader

An LSTM Recurrent Network for Step Counting

Ziyi Chen

Computer Science

University of California Santa Cruz

zchen139@ucsc.edu

Abstract

Smartphones with sensors such as accelerometer and gyroscope can be used as pedometers and navigators. In this paper, we propose to use an LSTM recurrent network for counting the number of steps taken by both blind and sighted users, based on an annotated smartphone sensor dataset, WeAllWork. The models were trained separately for sighted people, blind people with a long cane or a guide dog for Leave-One-Out training modality. It achieved 5% overcount and undercount rate.

1 Introduction

With the increasing ubiquity of smartphones, users are now carrying plenty of sensors with them such as accelerometer, gyroscope, magnetometer, wherever they go. Step counters are being integrated into an increasing number of portable consumer electronic devices such as music players, smartphones, and mobile phones (Wikipedia(2017a)). There are various of step counting apps on smartphones. Step counters can also be used for estimating the distance and the position in indoor pedestrian navigation systems, which is especially helpful not only for blind people but also for sighted people who need directional information in unfamiliar places.

In this paper, we propose an LSTM model trained with indoor walking sensor data from iPhones, and annotated data generated by shoe-mounted sensors (MetaWear-CPRO) from the WeAllWalk dataset, to predict the number of steps. The MetaWear-CPRO units are attached to the user's shoes so they can provide precise heel strike times. In the dataset, blind volunteers using a long cane or a guide dog and sighted volunteers have different gait patterns, so we built the mod-

els separately for each group of walkers and measured the performances based on three error metrics. We also tested the accuracy of those models by using leave-one-out cross-validation. Three error metrics splitting intervals differently were used for measuring the overcount and undercount rates of the system. We tried different parameters for the LSTM models such as the number of training steps and window size to find the best settings. The model achieved 1% overcount and undercount rate on a mixed dataset and 5% under the Stratified Leave-One-Out training modality.

2 Background and Related Work

2.1 Step Counting

Automatic step counting has received substantial attention in both research and commercial domains. There is a wealth of studies on the use of inertial sensors for detecting and characterizing walk-related activities. Pedometers are usually portable and electronic or electromechanical (Wikipedia(2017a)). They can be embedded in shoes, in smartwatches, in smartphones, and attached to users' ankles or hung on the belt.

(Brajdic and Harle(2013)) evaluated common walk detection (WD) and step counting (SC) algorithms applied to smartphone sensor data. The results favor the use of standard deviation thresholding (WD) and windowed peak detection (SC) with error rates of less than 3%. (Tomlein et al.(2012)Tomlein, Bielik, Kratky, Mitrik, Barla, and Bielikova) introduced step detection and intelligent detection of cheating based on smartphone sensors. (Naqvib et al.(2012)Naqvib, Kumar, Chauhan, and Sahni) presented a method for counting the number of steps taken by a user using the smartphone-based accelerometer while walking at any variable speed.

With the rapid development of deep learning, this advanced technology is used in vari-

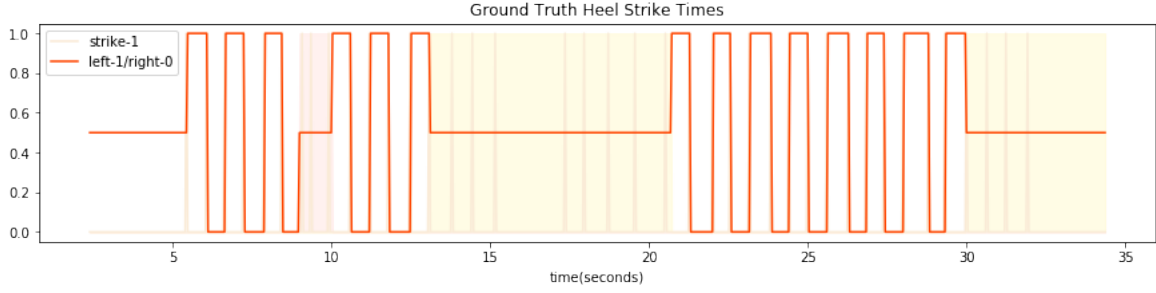


Figure 1: An example of heel strike times in T1_ID1_WC.xml from 2.4s to 34.4s. The first step at 5.4761s is a left step. A feature motion (the participant walked into the wall, stopped, and moved to the left) happened during 9.041862s to 10.041862s. Then one turn from east to south and another turn from south to east occurred during 13.1752s to 20.7419, and 30.0419s to 39.1419s respectively. Feature data, turn data, and all data recorded before the first step are removed.

ous fields including step counting. Since sensors provide time series data, researchers have tried to use RNN for counting the number of steps. (Edel and Koppe(2015)) uses Bidirectional Long Short-Term Memory Recurrent Neural Networks (BLSTM-RNNs) for step detection, step length approximation as well as heading estimation.

In addition to sighted people, some researchers also pay attention to people with visual impairment. (Haegle and Porretta(2015)) validated Centrios talking pedometer for adolescents with different level of visual impairment under the daily-living condition, while (Holbrook et al.(2011))Holbrook, Stevens, Kang, and Morgan) validated the same talking pedometer for adults.

2.2 The WeAllWalk Dataset

The WeAllWalk dataset (Flores and Manduchi(2016)) contains sensor data gathered from ten blind participants with a long cane or a guide dog and five sighted participants. The smartphone (iPhone 6s) carried by participants recorded the sensor data. Two small sensors attached to the participants shoes recorded heel strike times as the labels. Each segment of paths is marked as either a straight segment or a turn segment. Special circumstances on the road are also labeled as features. (Flores and Manduchi(2016)) have tested six different algorithms for step counting and turn detection.

3 Implementation

We propose an LSTM model trained with indoor walking sensor data from iPhone for step counting. Since blind participants using a long cane

or a guide dog and sighted volunteers have different gait patterns, we build the models separately and calculate the error rates by using three metrics. Also, we only consider straight segments in the paths, since the gait pattern is more likely to be regular than the gait pattern of turn segments, and remove segments marked as features such as opening a closed door and avoiding an obstacle. We try different parameters for the LSTM model and add a dropout layer to make the result more robust.

3.1 Data Preprocessing

We use two kinds of files from the dataset. The first type is CSV format iPhone sensor data. Each CSV file contains the sensor data recorded with a path and a person. There are 39 columns of sensor data and some of them are more useful than others. So we select 6 columns (rotationRateX, rotationRateY, rotationRateZ, userAccelerationX, userAccelerationY, userAccelerationZ) from the sensor data to building our model.

The second type is XML file containing annotated ground truth data for paths walked by each participant. Each file contains tags of start time, end time and direction for each segment the participant walked through. For each segment, the time and foot of each step are recorded, and special situation such as moving to the wall is also marked as feature with start time, end time and detailed description. We only train and test the step counting system with the segments recorded when participants traverse straight in each path, where gait patterns are assumed to be regular. We also remove time slots that have been marked as feature.

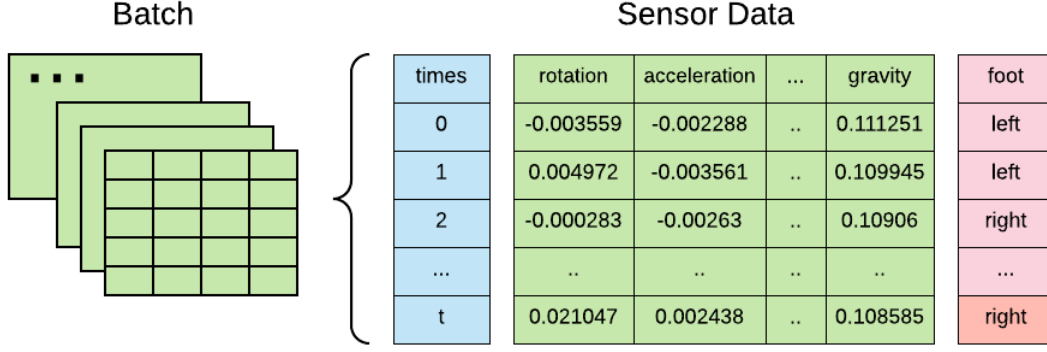


Figure 2: Input (green) and output (pink) samples for our model. The model uses the latest t records of the sensor data (green blocks) to predict the current status (the last pink block). The first $t-1$ predictions of each segment are from the intermediate outputs (light pink) of the recurrent neural network, since they do not have t records for prediction as the rest do.

Since the XML files only contain heel strike times and it's very difficult to predict heel strike times with the sensor data, we can not use them as the labels directly. If we regard the labels at heel strike times as 1s and the labels at other points in time as 0s, then the labels are too unbalanced to train a model to predict the labels at each point in time. So we transform the XML files to binary signals in which left steps toggle the signal from 0 to 1 and right steps toggle the signal from 1 to 0 as shown in Figure 1.

Finally, we windowed the data (window size is equal to the number of timesteps) for corresponding sensor data and ground truth signals to generate the formatted training data and labels.

3.2 The LSTM Model

Long short-term memory (LSTM) network is a time-recursive neural network, suitable for processing and predicting important properties of time series data. LSTM has many applications in the science and technology domains. LSTM-based systems can learn tasks such as translating natural languages, image analysis, speech recognition, controlling chat robots and so on.

LSTM network is a special kind of recurrent neural network (RNN). The main difference between LSTM and RNN lies in that LSTM adds a "processor" to judge whether the information is useful or not in the algorithm. The structure of this processor is called cell.

Three non-linear units (an input gate, a forget gate and an output gate) are placed in the cell. When a message enters the LSTM network, the system would determine whether the message is

useful or not. Only information that complies with algorithmic requirements will remain, and misleading information will be forgotten through the forget gate.

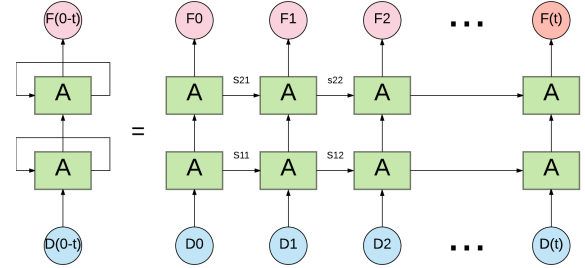


Figure 3: A two-layer LSTM recurrent network. Each green block is an LSTM cell. Blue circle $D(t)$ represents the sensor data recorded at time t while s is the inner LSTM state, and pink circle F is the output. Each LSTM cell receives the input of current sensor data and state from previous cell (the initial state is 0), and outputs a state and an output.

We use TensorFlow to implement the LSTM network. TensorFlow is an open-source software library that can be used for machine learning applications such as neural networks (Wikipedia(2017b)). It supports both CPU and GPU and it provides an interface in Python. TensorFlow uses a data flow graph to represent computation in terms of the dependencies between individual operations (TensorFlow(2017)). We first define the data flow graph and then create a session to run the graph. The saver class can save and restore the values of graph variable to and from checkpoints by mapping variable names to tensor

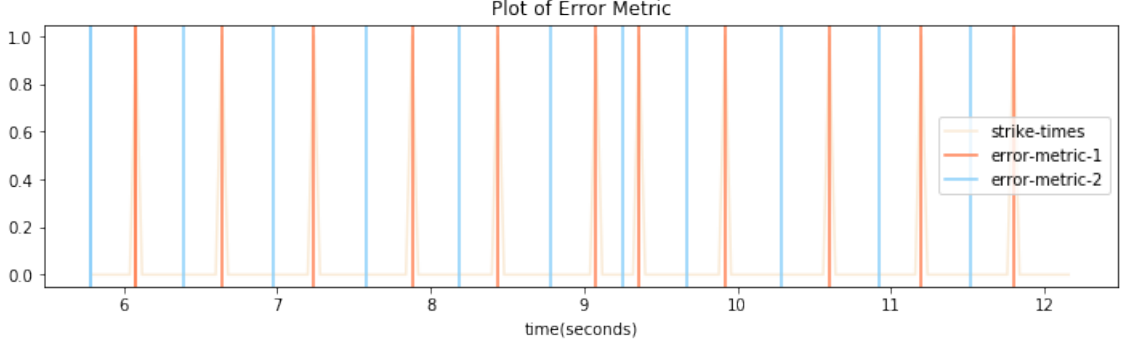


Figure 4: An example of three error metrics. Assume above plot is an entire segment. Error metric 1 (red line) divides segments into intervals exactly at each heel strike time. Error metric 2 (blue line) divides intervals at the center point of every pair of adjacent heel strike times. Both error metric 1 and 2 compute undercount and overcount rates for each interval independently while error metric 3 calculates undercount and overcount rates within the entire segment.

values.

As shown in Figure 3, a two-layer RNN network with 2 basic LSTM cells is built for training with mean squared error loss function. As shown in Figure 2, the input batch is a list of matrices. Each row of the matrices is a list of sensor data at a point in time. The length of the list is called the number of timesteps. For example, if we want to use the sensor data recorded at the latest 50 points in time to predict the current label, each sensor data contains input size (6 in our model) values of rotation rate and user acceleration in 3-dimension. So the matrix size is the number of timesteps multiply input size which is 50×6 . All such matrices form the input list and are transformed to tensor as the training data. Since the dataset is big and there are more than one hundred thousand elements in the input list which would make the training process very slow, we shuffle and divide training data into small batches (batch size = 256) and feed the batches to the optimizer one step by one step.

There are two ways to get the outputs. The first one is to use the latest 50 inputs to predict the current output. The second way is to use the intermediate outputs of RNN to generate predictions. The first one can not predict the first 50-1 labels, but it is more precise since more information is used to produce one output. We use the first way to predict all other labels.

3.3 Error Metrics

The original result signal is a list of float numbers around 0 to 1. Then we transform the signal into a binary signal where the value is either 0 or 1. And

the predicted heel strike times is the signal change times. Now we can calculate the accuracy rate of the result, which is the proportion of correct predictions (1 is predicted as 1 or 0 is predicted as 0) in total predictions. The error rate of the step counting model was measured using three different metrics as shown in Figure 4. The error metric 1 and 3 are as same as the error metrics proposed in (Flores and Manduchi(2016)).

The first metric splits intervals at each real heel strike times and counts the number of predicted steps within each time interval $[T_i, T_{i+1}]$. If exact one step is detected within each interval, the count of the step is correct. If no step is detected during the interval, then one undercount event happens. If n steps are detected during the interval, then $n - 1$ overcount events are recorded. The undercount and overcount rate is the number of undercount events or overcount events divided by the total number of real steps.

The second metric is similar to the first one, but it splits intervals at the center point of two adjacent ground-truth heel strike times, and counts the number of predicted steps within each time interval $[\frac{T_{i-1}+T_i}{2}, \frac{T_i+T_{i+1}}{2}]$. The undercount and overcount rate is calculated in a same way as the first metric does. As shown in Figure 15 at the end of this paper, the metric can decrease error rate when one step is detected slightly earlier ($t_i < T_i$) and the next step is detected sighted later ($t_{i+1} < T_{i+1}$). In this case, interval $[T_i, T_{i+1}]$ has one undercount event, and interval $[T_{i-1}, T_i]$ and $[T_{i+1}, T_{i+2}]$ have one overcount event.

The third metric counts the number of predicted

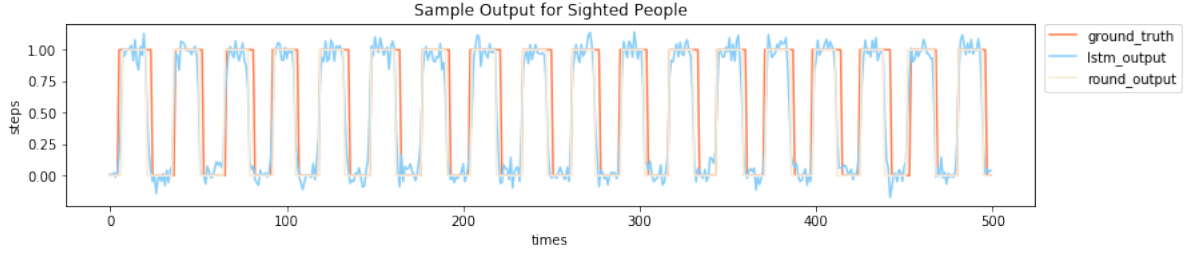


Figure 5: Sample output from mixed data for all sighted people. The origin output signal (blue line) swings near 0 or 1. The round signal (yellow line) is quite similar to the ground truth data (red line).

steps during each segment and compares to the number of ground-truth steps during the same segment. If the ground-truth number is larger, then undercount events happen. If the predicted number is larger, then overcount events happen. The undercount and overcount rate is calculated by dividing the sum of undercount events and overcount events by the number of all steps in ground truth. The undercount and overcount rate obtained by the error metric 3 is always smaller than or equal to the corresponding values computed by the metric 1 and 2.

4 Experiments

We preprocessed the WeAllWalk data to train the LSTM model for the different communities by using two ways of splitting training and testing data. The first way is to simply mix all data and split it into the training set and testing set. In this way, both the training and the testing data contain records from all participant and all segments. The second way is leaving one person out, which means testing set contains and only contains all records from one participant while the training set contains all other records from the remaining participants.

The model is trained with different sensor data, numbers of timesteps, output size, numbers of hidden layers, optimizers, learning rates and numbers of training steps. We first try different optimizers with various learning rates and find that AdamOptimizer with a learning rate around 0.01 can make the loss converged, and then fix the optimizer.

4.1 Sighted people

There are more than 120,000 valid records from sighted walkers, we split it into 100,000 records of training data and 25,000 records of testing data. Each input is a 3-dimensional tensor, with a shape

of batch size \times number of timesteps \times number of sensor signals.

For mixed data, we apply 10-fold cross-validation. A good result sample is shown in Figure 5. The output signal swings near 0 or 1. So it is reasonable to round the signal (> 0.5 turn to 1, ≤ 0.5 turn to 0). The rounded signal is similar to the ground truth data. However, not all results are as good as in this sample. Some of the bad results are shown at the end of the paper. Some results have a certain offset between the real heel strike time and the predicted heel strike time, some result curves shake more fiercely so that not all values are close to 0 or 1. There tend to be more strikes if the output value shakes around 0.5. So in our experiments, the overcount rate is always higher than the undercount rate.

Since there are 6 error rates, it is difficult to determine an overall measurement combining all error rates and tell which model is better. All 10 results are shown in Figure 6. The average undercount rate measured in metric 3 is around 0.6%, and the average overcount rate measured in metric 3 is around 1.4%. The average undercount rate measured in metric 2 is around 0.9%, and the average overcount rate measured in metric 2 is around 1.7%. The value of error rate is shown in table 2. The error rate measured in metric 1 is much higher than error rate measured in metric 2 and 3, the undercount rate measured in metric 1 is similar to overcount rate measured in metric 1 (around 20%) as shown in Figure 16. The reason that caused such situation is described in Figure 15. In metric 1, undercount and overcount error rates are similar since a undercount event is usually followed by a overcount event and vice versa.

For leave one person out method, the cross-validation result is shown in Figure 7. The average undercount rate in metric 3 is around 2.5%. The average overcount rate in metric 3 is around 7%.

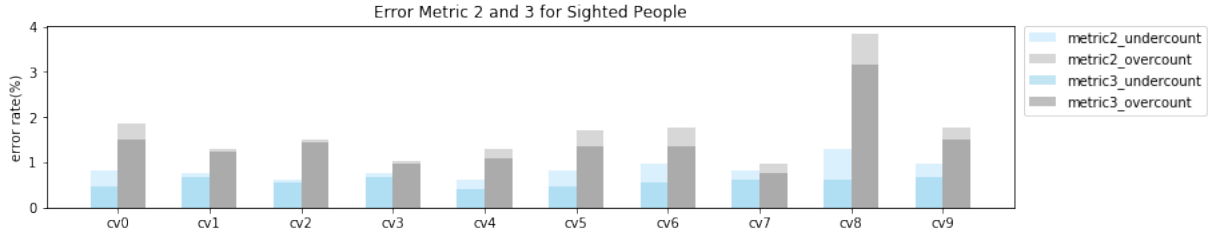


Figure 6: Error rates measured in error metric 2 and 3 under 10-fold cross-validation on mixed data for all sighted people. The error rate of metric 2 is always higher than metric 3. The undercount error rate (blue blocks) is less than overcount error rate (grey blocks). Detailed values are shown in table 2.



Figure 7: Error rates measured in error metric 1, 2 and 3 for leave-one-out data of sighted people.

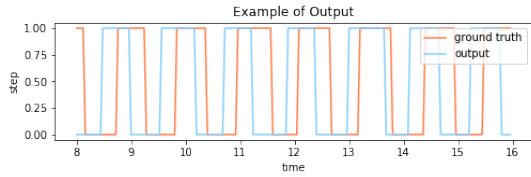


Figure 8: Sample output of offset. In this case, error metric 1 works better than error metric 2.

In some cases, metric 2 has bad performances, because there is an offset around half of each interval as shown in the Figure 9. In the experiments with different parameters of LSTM model, on some validation sets (cv3 performs best in most of the experiments) the model achieves overcount and undercount rates less than 0.1% in metric 3, while less than 1% in metric 1 or 2. But for other validation sets, the overcount rate is extremely high (30% to 60%). Each validation set has a better performance with models with different parameters. It might be because different people have different gait patterns. So I choose the model where each validation set has an average performance.

When both the training and testing data contain the sensor data from all people, the predicted signal is quite accurate, and the error rate (in metric

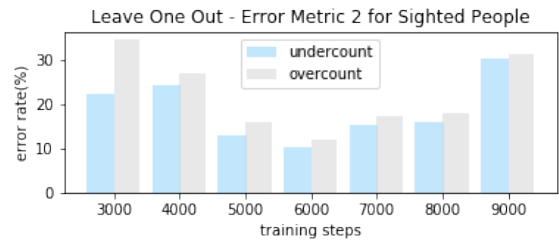


Figure 9: Error rates measured in metric 1 and 3 under 10-fold cross-validation with sighted people data. The error rate measured in metric 1 is always higher than in metric 3.

2 and 3) of step counting is small. However, with the leave-one-out method, there would be offsets for both training and testing data, and the accuracy of predicted signal is low. But the error rate in metric 1 could be small if the offset is similar for each heel strikes as shown in Figure 8.

4.2 Blind People with a long cane

There are more than 120,000 records from blind people with a long cane, participants 1, 2, 3, 5, 6, 7, 8 have sensor data for six paths. So we use data from participant 8 as the testing data, and records from all remaining people as the training

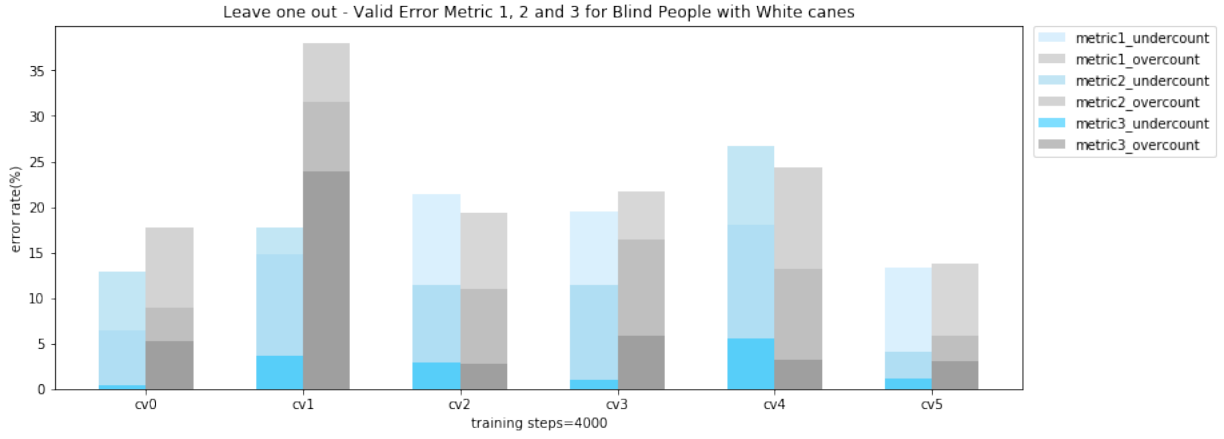


Figure 10: Error rates on blind people with a long cane leave-one-out validation set.

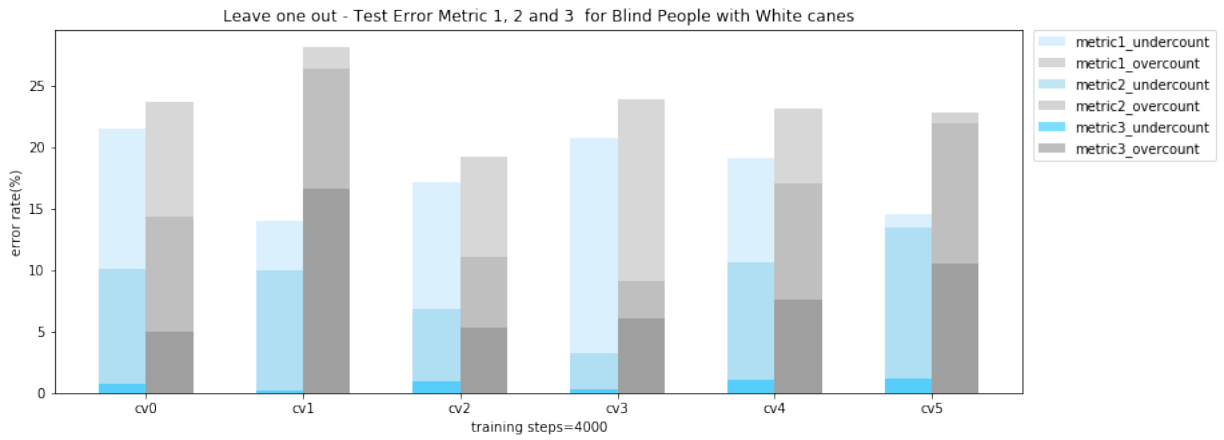


Figure 11: Error rates on blind people with a long cane leave-one-out testing set.

and validation data for 6-fold leave-one-out cross-validation. The validation and testing results are shown in Figure 10 and 11. All error rates are higher than on the mixed data. The good performance from the validation data does not mean that the model can have a good performance on the testing data. The training dataset only contains data from 6 different people, which is not a big number. If we have annotated data from more people, the LSTM model might detect more walking patterns of blind people and provide a better result.

4.3 Blind people using a guide dog

There are only 3 people walking with a guide dog. Each of them generates 30,000 records of sensor data. So we regard the data from two people as the training data and those from the left one as the testing data. The result is bad as shown in 12. Although the model shows a good performance on mixed data (error rate is around 5% in metric 2 and 2% in metric 3), it is difficult to predict the

Table 1: Error rates on blind people with a guide dog

error(%)		valid	test
metric1	undercount	23.90	10.18
	overcount	26.14	25.75
metric2	undercount	22.56	12.27
	overcount	29.03	19.49
metric3	undercount	4.52	0.53
	overcount	10.98	17.75

strike heel times of a person with a model trained with the data from only one other person.

5 Conclusion and Future Work

We trained an LSTM model using annotated smartphone sensor data from the WeAllWalk dataset to count steps. In the dataset, blind volunteers using a long cane or a guide dog, sighted volunteers have different gait patterns, so we sep-

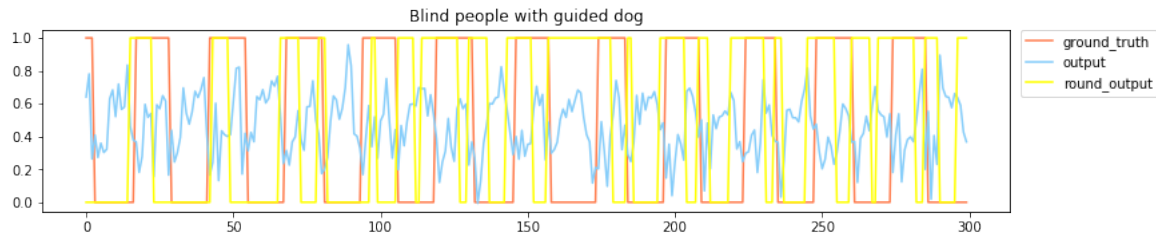


Figure 12: Sample output on blind people with guide dog.

arately built the models and calculated the error rates in three metrics. We also applied leave-one-out pedometers to test the accuracy of our models by using three error metrics, that split intervals differently to compute the number of overcounted and undercounted steps. The model achieved 1% overcount and undercount rate on the mixed training data and 5% under leave-one-out training modality.

As shown in Figure 14 and Figure 13, simply rounding the origin output signal might cause overcount or undercount event. So we can use a better way to transform the signal into a binary signal. In this paper, we only use the data of straight segments by removing turn segments and other features. We could consider turn segments and feature motions in the future. We now only use rotation rate and user acceleration as the input, we can also try more features in the dataset in the future.

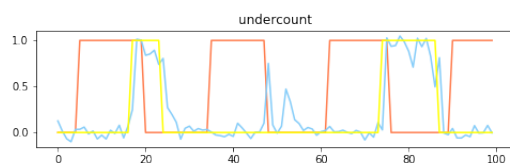


Figure 13: Sample of undercounting.

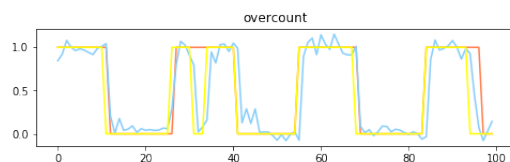


Figure 14: Sample of overcounting.

References

Dragan Ahmetovic, Cole Gleason, Chengxiong Ruan, Kris Kitani, Hironobu Takagi, and Chieko Asakawa.

2016. Navcog: a navigational cognitive assistant for the blind. In *Proceedings of the 18th International Conference on Human-Computer Interaction with Mobile Devices and Services*. ACM, pages 90–99.

Heikki J Ailisto, Mikko Lindholm, Jani Mantyjarvi, Elena Vildjiounaite, and Satu-Marja Makela. 2005. Identifying people from gait pattern with accelerometers. In *Proc. SPIE*. volume 5779, pages 7–14.

Moustafa Alzantot and Moustafa Youssef. 2012. Up-time: Ubiquitous pedestrian tracking using mobile phones. In *Wireless Communications and Networking Conference (WCNC), 2012 IEEE*. IEEE, pages 3204–3209.

Agata Brajdic and Robert Harle. 2013. Walk detection and step counting on unconstrained smartphones. In *Proceedings of the 2013 ACM international joint conference on Pervasive and ubiquitous computing*. ACM, pages 225–234.

Meredith A Case, Holland A Burwick, Kevin G Volpp, and Mitesh S Patel. 2015. Accuracy of smartphone applications and wearable devices for tracking physical activity data. *Jama* 313(6):625–626.

James Coughlan, Roberto Manduchi, and Huiying Shen. 2006. Cell phone-based wayfinding for the visually impaired. In *1st International Workshop on Mobile Vision*. pages 1–15.

Marcus Edel and Enrico Koppe. 2015. An advanced method for pedestrian dead reckoning using blstm-rnns. In *Indoor Positioning and Indoor Navigation (IPIN), 2015 International Conference on*. IEEE, pages 1–6.

German H Flores and Roberto Manduchi. 2016. Weall-walk: An annotated data set of inertial sensor time series from blind walkers. In *Proceedings of the 18th International ACM SIGACCESS Conference on Computers and Accessibility*. ACM, pages 141–150.

Felix A Gers, Jurgen Schmidhuber, and Fred Cummins. 1999. Learning to forget: Continual prediction with lstm .

Justin A Haegele and David L Porretta. 2015. Validation of a talking pedometer for adolescents with visual impairments in free-living conditions. *Journal of Visual Impairment & Blindness* 109(3):219–223.

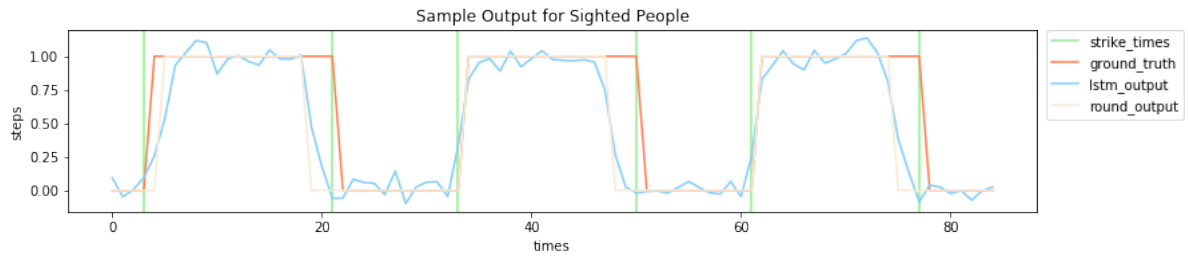


Figure 15: A bad sample in error metric 1. The green line splits the intervals in error metric 1. There are random offsets between actual strike times and predicted strike times. In this case, the first, third and fifth interval has one overcount while the second and the fourth intervals have one undercount.

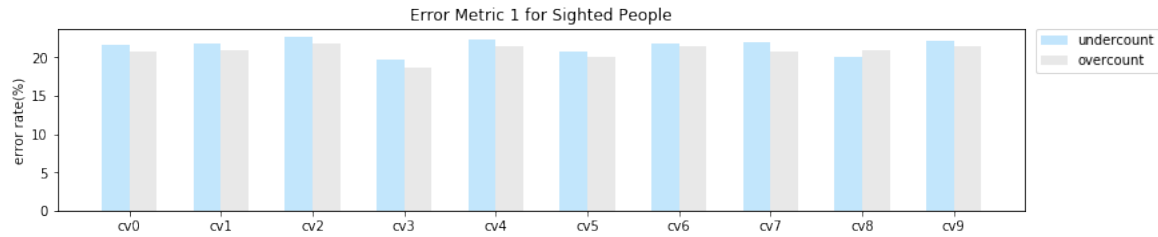


Figure 16: Error metric 1 under 10-fold cross-validation on sighted people. The error rate is much higher than the error rate in metric 2 and 3 as shown in this figure. The reason that caused such situation is also described in tge figure.

Ann Halleman, Els Ortibus, Françoise Meire, and Peter Aerts. 2010. Low vision affects dynamic stability of gait. *Gait & posture* 32(4):547–551.

Elizabeth Ackley Holbrook, Sandy L Stevens, Minsoo Kang, and Don W Morgan. 2011. Validation of a talking pedometer for adults with visual impairment. *Medicine & Science in Sports & Exercise* 43(6):1094–1099.

Sampath Jayalath, Nimsiri Abhayasinghe, and Iain Murray. 2013. A gyroscope based accurate pedometer algorithm. In *International Conference on Indoor Positioning and Indoor Navigation*, volume 28, page 31st.

Andrea Mannini and Angelo Maria Sabatini. 2011. A hidden markov model-based technique for gait segmentation using a foot-mounted gyroscope. In *Engineering in Medicine and Biology Society, EMBC, 2011 Annual International Conference of the IEEE*. IEEE, pages 4369–4373.

Najme Zehra Naqvib, Ashwani Kumar, Aanchal Chauhan, and Kritika Sahni. 2012. Step counting using smartphone-based accelerometer. *International Journal on Computer Science and Engineering* 4(5):675.

Thomas Olutoyin Oshin and Stefan Poslad. 2013. Ersp: An energy-efficient real-time smartphone pedometer. In *Systems, Man, and Cybernetics (SMC), 2013 IEEE International Conference on*. IEEE, pages 2067–2072.

TensorFlow. 2017. Programmer’s guide - graphs and sessions. https://www.tensorflow.org/programmers_guide/graphs. [Online; accessed 14-December-2017].

Michal Tomlein, Pavol Bielik, Peter Kratky, Stefan Mitrik, Michal Barla, and Maria Bielikova. 2012. Advanced pedometer for smartphone-based activity tracking. In *HEALTHINF*, pages 401–404.

Wikipedia. 2017a. Pedometer wikipedia, the free encyclopedia. <https://en.wikipedia.org/wiki/Pedometer>. [Online; accessed 14-December-2017].

Wikipedia. 2017b. Tensorflow — Wikipedia, the free encyclopedia. <https://en.wikipedia.org/wiki/TensorFlow>. [Online; accessed 14-December-2017].

Wojciech Zaremba, Ilya Sutskever, and Oriol Vinyals. 2014. Recurrent neural network regularization. *arXiv preprint arXiv:1409.2329*.

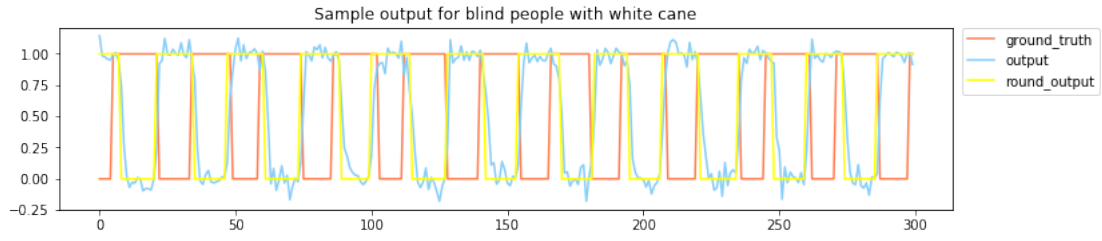


Figure 17: An output sample on blind people with a long cane.

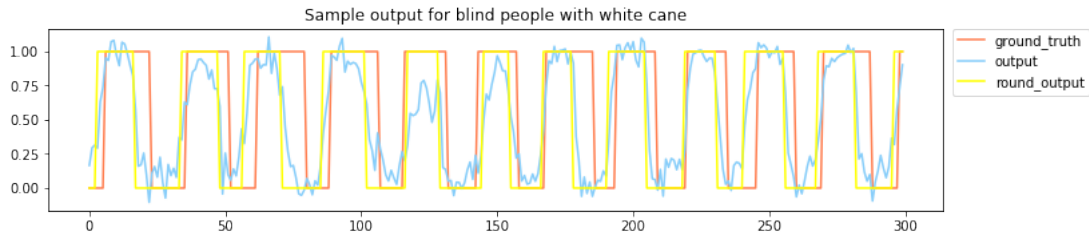


Figure 18: An output sample on blind people with a long cane.

Table 2: Performance measured in metric 2 and 3 under 10-fold cross-validation on sighted people

error(%)		cv0	cv1	cv2	cv3	cv4	cv5	cv6	cv7	cv8	cv9
metric1	undercount	0.82	0.75	0.62	0.75	0.62	0.82	0.96	0.82	1.3	0.96
	overcount	1.85	1.3	1.5	1.03	1.3	1.71	1.78	0.96	3.83	1.78
metric2	undercount	0.48	0.68	0.55	0.68	0.41	0.48	0.55	0.62	0.62	0.68
	overcount	1.5	1.23	1.44	0.96	1.09	1.37	1.37	0.75	3.15	1.5

Table 3: Performance measured in mertric 1, 2 and 3 on blind people using a long cane

error(%)		cv0		cv1		cv2		cv3		cv4		cv5	
		valid	test	valid	test	valid	test	valid	test	valid	test	valid	test
m1	undercount	6.44	21.49	14.83	14.03	21.45	17.1	19.5	20.67	18.05	19.03	13.35	14.56
	overcount	8.87	23.63	31.5	28.1	19.32	19.2	21.69	23.91	13.17	23.09	13.7	21.94
m2	undercount	12.93	10.09	17.79	9.97	11.36	6.77	11.49	3.28	26.69	10.62	4.09	13.45
	overcount	17.81	14.36	38.01	26.33	10.97	11.07	16.37	9.06	24.35	17.06	5.9	22.76
m3	undercount	0.43	0.7	3.63	0.21	2.94	0.94	1.03	0.29	5.59	1.11	1.2	1.19
	overcount	5.32	4.96	23.85	16.57	2.7	5.25	5.9	6.07	3.25	7.55	3.01	10.5